Planning of arrival and departure routes in terminal maneuvering area based on high dimensionality reduction environment modeling method

基于高维度降低环境建模方法的终端区起降航线规划

Siyu Su[1]· Youchao Sun[1]®· Chong Peng [1]· Haiyun Yang [1] Received: 28 July 2020 / Revised: 15 September 2020 / Accepted: 23 September 2020 / Published online: 13 October 2020

Siyu Su[1]· Youchao Sun[1]®· Chong Peng [1]· Haiyun Yang [1] 收到日期:2020 年 7 月 28 日 / 修订日期:2020 年 9 月 15 日 / 接受日期:2020 年 9 月 23 日 / 在线发布日期:2020 年 10 月 13 日

Abstract

The efficient design of arrival and departure routes in the terminal maneuvering area plays a key role in increasing airport capacity and reducing traffic congestion. In our study, we establish an arrival and departure route planning model in the terminal maneuvering area, taking into account the airspace environmental constraints and aircraft operational constraints. Then the three-dimensional environment modeling method with a high degree of dimensionality reduction is introduced to improve the efficiency of route planning, and routes are planned sequentially using the A* algorithm in a dimensionally reduced environment. Numerical simulation tests, performed on the terminal maneuvering area of Chengdu Shuangliu Airport in China, show the effectiveness of the proposed method. Each route is given two planning schemes considering the maximum and minimum takeoff or descent slope, and a total of seven routes is generated.

摘要

终端区起降航线的有效设计对于提高机场容量和减少交通拥堵起着关键作用。在研究中，我们建立了考虑空域环境约束和飞机运行约束的终端区起降航线规划模型。然后引入了三维环境建模方法，该方法具有高度维度降低，以提高航线规划效率，并在降维环境中使用 A* 算法顺序规划航线。在中国成都双流机场的终端区进行的数值仿真测试显示了提出方法的有效性。每个航线都考虑了最大和最小起飞或下降坡度的两种规划方案，共生成了七条航线。

Keywords Terminal maneuvering area · Arrival and departure routes · High dimensionality reduction · A* algorithm · Takeoff/descent slope

关键词终端区 · 起降航线 · 高维度降低 · A* 算法 · 起飞/下降坡度

1 Introduction

1 引言

A terminal Maneuvering Area (TMA) is an area consisting of one or more adjacent airports in which both the takeoff and the landing phases of the aircraft occur. Intensive airport layout, complex airspace structure, and rapidly growing air traffic flow make the TMA more congested. The standard terminal arrival routes (STARs) and standard instrument departure routes (SIDs) planning, as the core content of the TMA airspace planning, play an important role in reducing the operational complexity of the airspace and achieving safe and efficient flight of the aircraft. Currently, the STARs and SIDs planning are mainly based on manual design, and the efficiency is relatively low. This kind of design is difficult to meet the increasing air traffic demand and the economics and safety of aircraft operation. Therefore, the objective of this study is to automatically plan STARs and SIDs concerning certain constraints.

终端机动区 (TMA) 是由一个或多个相邻机场组成的区域，在其中飞机的起飞和降落阶段都会发生。密集的机场布局、复杂的空域结构和快速增长的航空流量使得 TMA 变得更加拥挤。标准的终端进近路线 (STARs) 和标准仪表离场路线 (SIDs) 的规划，作为 TMA 空域规划的核心内容，在降低空域的运营复杂性以及实现飞机的安全和高效飞行方面发挥着重要作用。目前，STARs 和 SIDs 的规划主要基于手工设计，效率相对较低。这种设计难以满足日益增长的航空交通需求以及飞机运营的经济性和安全性。因此，本研究的目标是自动规划考虑特定约束的 STARs 和 SIDs。

The design of STARs and SIDs belongs to the category of path planning, that is, in a fixed environment, finding a collision-free optimal path from the starting point to the ending point. Contrary to trajectory design, route planning does not involve any notion of time. Research on path planning has been around for many years, it can be divided into two-dimensional (2D) path planning [1, 2] and three-dimensional (3D) path planning [3, 4] , single path planning [5] and multiple path planning [6] from different perspectives. Especially in the field of robotics, the fruitful research results have been achieved [7-9]. Researchers usually use the global deterministic environment to represent the link graph with weights and use the mature ant colony algorithm and A* algorithm to solve the problem. However, to our knowledge, there are few studies on the planning of STARs and SIDs in TMA. In [10], the author combined the actual operational data of the airport and used the A*-1 algorithm to realize 3D planning of terminal routes under uncertain weather. Since the method used the fitted vertical profile data to indicate the vertical characteristics of the route, the accuracy of the results is not satisfactory. In [11], STARs and SIDs were designed using a fast matching algorithm, but the takeoff and descent slope of aircraft were not specifically considered. In [12], the single route was designed by the method of Branch and Bound. The researchers regarded the airspace obstacle as a cylinder, and the aircraft bypassed the obstacle clockwise or counterclockwise or imposing a level flight. In [13], a Simulated Annealing algorithm was used to generate multiple STARs and SIDs, taking obstacle avoidance and route separation as the main constraints. However, the researchers paid little attention to the order of terminal routes planning. In [14, 15], the design of terminal routes was divided into two parts, horizontal design, and vertical design. The horizontal design was used to address obstacles and special-use airspace areas avoidance, the vertical planning was used to deal with the takeoff and descent slope of aircraft. Although this approach improves the efficiency of route planning, it may lose some feasible solution because obstacle avoidance can only choose to fly around instead of a flyover.

STARs 和 SIDs 的设计属于路径规划的范畴，即在固定环境中，找到从起点到终点的无碰撞最优路径。与轨迹设计不同，路线规划不涉及时间的概念。路径规划的研究已经进行了许多年，它可以分为二维 (2D) 路径规划 [1, 2] 和三维 (3D) 路径规划 [3, 4] ，从不同的角度还可以分为单一路径规划 [5] 和多路径规划 [6]。特别是在机器人领域，已经取得了丰富的研究成果 [7-9]。研究人员通常使用全局确定性环境来表示带权重的链接图，并使用成熟的蚁群算法和 A* 算法来解决问题。然而，据我们所知，关于在 TMA 中规划 STARs 和 SIDs 的研究较少。在 [10] 中，作者结合了机场的实际运行数据，并使用 A*-1 算法在不确定天气条件下实现终端路线的 3D 规划。由于该方法使用拟合的垂直剖面数据来指示路线的垂直特性，因此结果的准确性不令人满意。在 [11] 中，使用快速匹配算法设计了 STARs 和 SIDs，但没有特别考虑飞机的起飞和下降坡度。在 [12] 中，通过分支限界法设计了单一路线。研究人员将空域障碍视为圆柱体，飞机绕障碍顺时针或逆时针飞行，或者进行水平飞行。在 [13] 中，使用模拟退火算法生成了多个 STARs 和 SIDs，将避障和路线分离作为主要约束。然而，研究人员对终端路线规划顺序的关注较少。在 [14, 15] 中，终端路线的设计被分为两部分，水平设计和垂直设计。水平设计用于处理障碍物和特殊使用空域的规避，垂直规划用于处理飞机的起飞和下降坡度。尽管这种方法提高了路线规划的效率，但它可能会丢失一些可行解，因为避障只能选择绕飞而不是飞越。

In our research, we propose a 3D environmental modeling method based on a high degree of dimensionality reduction to deal with complex airspace environments in TMA. To satisfy airspace environmental constraints (obstacle and special-use airspace area avoidance) and aircraft operational constraints (takeoff/descent slope and turning angle of the aircraft), the terminal route planning model which minimizes the route lengths is established. Accurate or heuristic methods can be applied to solve the planning model, but the exact model may not find a solution or is very time-consuming, so the heuristic method A* algorithm is used to design the route. The 3D airspace environment is rasterized and reduced to a two-dimensional plane with dimensionality reduction methods. Design the cost function of the A* algorithm and perform route planning on the reduced 2D plane. Since the dimensionality-reduced airspace environment reduces the number of rasters and the A* algorithm has a high search efficiency, it can meet the efficiency requirements of the planning algorithm while ensuring the accuracy of the environment description, which compensates for the shortcomings of the traditional raster method. In addition, a 2D plane generated by the high degree of dimensionality reduction method is used as the environment model for route planning, the plane ignores some of the obstacles that are low in height and have no effect on

☒ Youchao Sun
☒ 孙宇超
18851871550@163.com
1 College of Civil Aviation, Nanjing University of Aeronautics and Astronautics, No. 29, Yudao St, Nanjing 210016, China
1 南京航空航天大学民航学院，南京市御道街 29 号，210016，中国

the flight path of the aircraft, avoiding unnecessary calculations.

在我们的研究中，我们提出了一种基于高维降维的 3D 环境建模方法，用于处理 TMA 中的复杂空域环境。为了满足空域环境约束 (避开障碍物和特殊用途空域) 以及飞机运行约束 (起飞/降落坡度和飞机转弯角度)，建立了最小化航线长度的终端航线规划模型。可以应用精确或启发式方法解决规划模型，但由于精确模型可能找不到解决方案或非常耗时，因此使用启发式方法 A* 算法来设计航线。3D 空域环境通过降维方法被栅格化并简化为二维平面。设计 A* 算法的成本函数，并在降维后的 2D 平面上进行航线规划。由于降维后的空域环境减少了栅格数量，且 A* 算法具有高搜索效率，它可以在确保环境描述准确性的同时满足规划算法的效率要求，弥补了传统栅格方法的不足。此外，使用高度降维方法生成的 2D 平面作为航线规划的环境模型，该平面忽略了一些对飞机航迹无影响的高度较低的障碍物，避免了不必要的计算。

This paper is organized as follows. Section 2 introduces the STARs and SIDs planning model. Section 3 explains the method of solving the problem, including 3D high degree of dimensionality reduction environment modeling method and A* algorithm. Section 4 presents the simulation results. Section 5 draws conclusions and proposes future research directions.

本文的组织结构如下。第 2 节介绍了 STARs 和 SIDs 规划模型。第 3 节解释了求解问题的方法，包括 3D 高维降维环境建模方法和 A* 算法。第 4 节展示了模拟结果。第 5 节得出结论并提出未来的研究方向。

2 Problem description and modeling

2 问题描述与建模

2.1 Problem description

2.1 问题描述

As the aircraft flight state transition area, TMA is one of the most complex airspace types, and its number and layout of the terminal area have an important impact on the design of STARs and SIDs. There are many limitations in TMA that need to be satisfied, which are mainly divided into two categories: aircraft operational constraints (such as obstacle avoidance, flyable segments) and environmental constraints (such as aircraft noise abatement). These constraints in TMA make route planning more difficult. In this paper, the panning of STARs and SIDs under the premise of the known route start and end points, a STAR is a route connecting the last en-route waypoint to the initial approach fix (IAF), and a SID is a flight route that an aircraft takes off from the airport until the start of an en-route phase.

作为飞机飞行状态转换区域，终端机动区 (TMA) 是最复杂的空域类型之一，其数量和布局对标准到达程序 (STARs) 和标准离场程序 (SIDs) 的设计具有重要影响。TMA 中存在许多需要满足的限制，主要分为两类: 飞机操作约束 (如避障、可飞行段) 和环境约束 (如飞机降噪)。TMA 中的这些约束使得航线规划更加困难。本文在已知航线起点和终点的前提下，讨论了 STARs 和 SIDs 的规划，STAR 是指连接最后一个航路点与初始进近定位点 (IAF) 的航线，而 SID 是指飞机从机场起飞直到航路阶段开始的飞行航线。

2.2 TMA Environment modeling

2.2 TMA 环境建模

The 3D rectangular coordinate system is established around the airport, and the 3D airspace model is constructed according to the airspace environment in TMA, as shown in Fig. 1.

在机场周围建立三维直角坐标系，并根据 TMA 中的空域环境构建三维空域模型，如图 1 所示。

The airspace units include:

空域单元包括:

(1) Obstacle. $O(M)$ is a set of obstacles with M obstacles, each obstacle $\Omega_j = (x_j, y_j, z_j), j = 1, 2, \ldots, M.$ (x_j, y_j) is the horizontal coordinate of the obstacle Ω_j , and z_j is the height of Ω_j ;

(1) 障碍物。$O(M)$ 是一个包含 M 个障碍物的障碍物集合，每个障碍物 $\Omega_j = (x_j, y_j, z_j), j = 1, 2, \ldots, M.$ (x_j, y_j) 是障碍物的水平坐标 Ω_j ， z_j 是 Ω_j 的高度;

(2) Special use airspace area, including Prohibited Area, Restricted Area, and Dangerous Area, referred to as PRD. These three airspace types are regarded as aircraft nonflyable airspace [16]. $U(t)$ is a PRD set, which has a total of t special use airspace areas;

(2) 特殊使用空域区域，包括禁飞区、限制区和危险区，统称为 PRD。这三种空域类型被视为飞机不可飞行的空域 [16]。$U(t)$ 是一个 PRD 集合，共有 t 个特殊使用空域区域；

(3) Runway. The runway is represented by the rectangle of the midpoint at the origin of the coordinate, the direction of the runway is consistent with the runway's true orientation.

(3) 跑道。跑道由坐标原点中点的矩形表示，跑道的方向与跑道的真实方向一致。

The length of the runway is l_R , and the runway number is n_R ;

跑道的长度是 l_R ，跑道的编号是 n_R ；

(4) The total number of routes to be planned. Set up a total of N routes;

(4) 需要规划的总航线数。设置总共 N 条航线；

(5) The start point. Let the start point of a route be $A_i = \left({A_x}^i, {A_y}^i, {A_z}^i\right), i = 1, 2, \ldots, N$, the start point of a SID is the departure end of the runway (DER), and the start point of a STAR is the last en-route waypoint;

(5) 起点设定。让一条航线的起点为 $A_i = \left({A_x}^i, {A_y}^i, {A_z}^i\right), i = 1, 2, \ldots, N$ ，SID 的起点是跑道起飞端 (DER)，STAR 的起点是最后一个航路导航点；

(6) The end point. Let the endpoint of a route be $B_i = \left({B_x}^i \ , \ {B_y}^i, {B_z}^i\right), i = 1, 2, \ldots, N$, the end point of a SID is the start point of en-route, and the end point of a STAR is IAF; (7) takeoff/descent slope. Due to the specification and capabilities of aircraft using the routes can vary significantly, there are different takeoff and descent slopes. Let the minimum takeoff slope be $\alpha_{\min,\mathrm{TO}}$, the maximum takeoff slope be $\alpha_{\max,\mathrm{TO}}$, the minimum descent slope be $\alpha_{\min,\mathrm{LD}}$, and the maximum descent slope be $\alpha_{\max,\mathrm{LD}}$.

(6) 终点设定。让一条航线的终点为 $B_i = \left({B_x}^i \ \ {B_y}^i, {B_z}^i\right), i = 1, 2, \ldots, N$ ，SID 的终点是航路起点，STAR 的终点是初始进近定位点 (IAF)；(7) 起飞/下降坡度。由于使用航线的飞机规格和能力可能会有很大差异，因此有不同的起飞和下降坡度。让最小起飞坡度为 $\alpha_{\min,\mathrm{TO}}$ ，最大起飞坡度为 $\alpha_{\max,\mathrm{TO}}$ ，最小下降坡度为 $\alpha_{\min,\mathrm{LD}}$ ，最大下降坡度为 $\alpha_{\max,\mathrm{LD}}$ 。

Fig. 1 Schematic diagram of the 3D airspace model in TMA

图 1 TMA 中三维空域模型的示意图

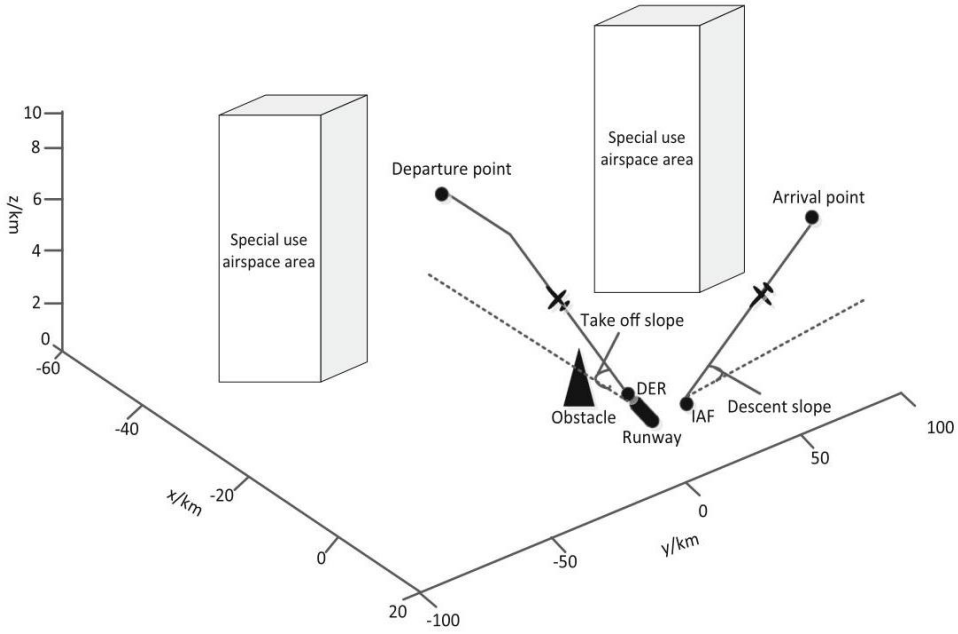

2.3 STARs and SIDs planning modeling

2.3 STARs 和 SIDs 规划建模

2.3.1 Objective function

2.3.1 目标函数

The length of the route is the main factor affecting the economics of STARs and SIDs planning. For each route $\gamma_i, i = 1, 2, \ldots, N$, the length of the route is $L_{\gamma i}$, and the total length of the route denotes as:

航线的长度是影响 STARs 和 SIDs 规划经济性的主要因素。对于每条航线 $\gamma_i, i = 1, 2, \ldots, N$ ，航线的长度是 $L_{\gamma i}$ ，航线的总长度表示为:

$$L = \sum_{i=1}^{N} L_{\gamma_i} \tag{1}$$

2.3.2 Constraints

2.3.2 约束条件

(1) Obstacle avoidance.

(1) 避障。

When the aircraft is flying along the route, it must keep a certain distance from the ground obstacles, horizontally bypassing or flying over.

当飞机沿着航线飞行时，它必须与地面障碍物保持一定的距离，水平绕行或飞越。

$$\gamma_i \cap O\left(M\right) = \varnothing, i = 1, 2, \ldots, N \tag{2s}$$

(2) Special use airspace area avoidance

(2) 特殊使用空域避让

When the special use airspace area exists in the airport airspace environment, the departure and arrival route cannot pass through such airspace. Regarding the height of the special use airspace area as infinitely high, the aircraft can only fly around it.

当特殊使用空域存在于机场空域环境中时，起飞和降落航线不能穿过此类空域。将特殊使用空域的高度视为无限高，飞机只能绕行。

$$\gamma_i \cap U\left(t\right) = \varnothing, i = 1, 2, \ldots, N \tag{3}$$

(3) Aircraft operational constraints

(3) 飞机操作约束

a. Aircraft turning angle:

a. 飞机转弯角度:

$$\frac{\pi}{2} \leq \beta \leq \frac{3\pi}{2} \tag{4}$$

b. Aircraft takeoff slope:

b. 飞机起飞坡度:

$$\alpha_{\min,\mathrm{TO}} \leq \alpha_{\mathrm{TO}} \leq \alpha_{\max,\mathrm{TO}} \tag{5}$$

c. Aircraft descent slope:

c. 飞机下降坡度:

$$\alpha_{\min,\mathrm{LD}} \leq \alpha_{\mathrm{LD}} \leq \alpha_{\max,\mathrm{LD}} \tag{6}$$

In summary, the STARs and SIDs model can be expressed as:

总结来说，STARs 和 SIDs 模型可以表示为:

$$\begin{cases} \min\left(\sum_{i=1}^{N} L_{\gamma_i}\right) \\ \text{s.t } \gamma_i \cap O\left(M\right) = \varnothing, i = 1, 2, \ldots, N \\ \gamma_i \cap U\left(t\right) = \varnothing, i = 1, 2, \ldots, N \\ \frac{\pi}{2} \leq \beta \leq \frac{3\pi}{2} \\ \alpha_{\min}\alpha_{\max} \odot \alpha_{\max}, T\alpha_i \leq \alpha_{\max}, T\alpha_i \leq \alpha_{\max}, T \end{cases} \tag{7}$$

3 Solution approaches

3 解决方案方法

The terminal airspace environment is rasterized by referring to the unit decomposition modeling method of the UAV path planning. In the case of ensuring accuracy, if the traditional raster method is directly used to solve STARs and SIDs planning model in a 3D environment, the number of grids will be very large, and the route planning efficiency will be greatly reduced. To reduce the number of grids in the solving process, a 3D environment rasterization method based on a high degree of dimensionality reduction is adopted in this paper to transform the 3D environment into the 2D environment.

通过参考无人机路径规划的单元分解建模方法，对终端空域环境进行栅格化。在确保精度的前提下，如果直接使用传统的栅格方法在三维环境中解决 STARs 和 SIDs 规划模型，网格数量将会非常大，路径规划效率将大大降低。为了在解决过程中减少网格数量，本文采用了一种基于高度降维的三维环境栅格化方法，将三维环境转换为二维环境。

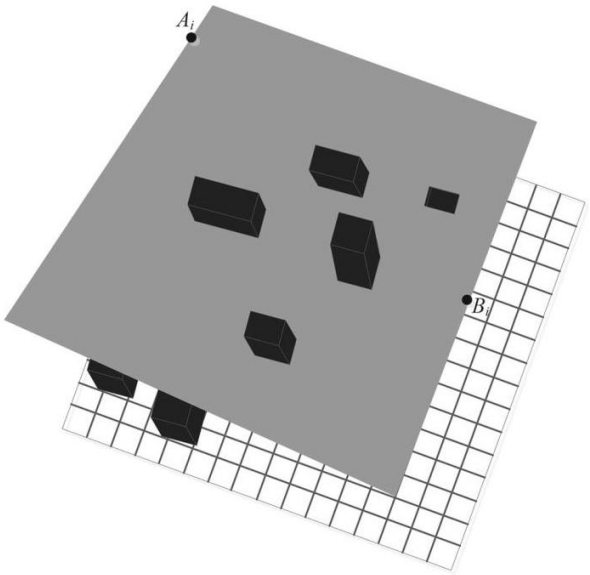

Fig. 2 Establishing an S -plane
图 2 建立一个 S 平面

3.1 High dimensionality reduction rasterization process

3.1 高维度降低栅格化过程

Step 1: The traditional grid method is used to process the airspace environment of the TMA involved in 2.2, and the 3D airspace environment is divided into m $*$ m $*$ m grids. The grid setting with obstacles is 1, indicated by dark colors, and the grid without obstacles is set to 0, indicated by light colors. The grids of the special use airspace area are all set to 1, and the height is the same as that of the rasterized airspace environment. The coordinates of each unit raster are the center of the grid.

第一步: 使用传统的网格方法处理 2.2 节中涉及的 TMA 空域环境, 并将三维空域环境划分为 m∗ m∗ m 格网。设置有障碍物的网格为 1，用深色表示；无障碍物的网格设置为 0，用浅色表示。特殊用途空域区域的格网均设置为 1，高度与栅格化的空域环境相同。每个单元栅格的坐标是网格的中心。

Step 2: The S -plane perpendicular to the YOZ -plane is generated by crossing the starting point A_i and ending point B_i of the terminal routes, as shown in Fig. 2. S -plane crosses the starting point A_i and ending point B_i , and cuts through obstacles higher than S -plane and all the special use airspace area in the airspace environment.

第二步: 生成垂直于 YOZ 平面的 S 平面，该平面通过终端航路的起点 A_i 和终点 B_i ，如图 2 所示。S 平面穿过起点 A_i 和终点 B_i ，并切割高于 S 平面以及空域环境中所有特殊用途空域区域的障碍物。

Step 3: Rasterize the 2DS -plane generated in Step 2. The essence of the S -plane rasterization is to project the XOY-plane into S -plane. The size of the grid in the S -plane depends on the size of the XOY-plane grid and the angle between the S -plane and the XOY-plane. The grids with the obstacles' height higher than the S -plane and those in the special use airspace area are regarded as obstacle grids and the rest as free grids.

第三步: 栅格化第 2 步中生成的 2DS 平面。S 平面栅格化的本质是将 XOY 平面投影到 S 平面。S 平面中网格的大小取决于 XOY 平面网格的大小以及 S 平面与 XOY 平面之间的角度。高于 S 平面障碍物高度的网格以及特殊用途空域区域内的网格被视为障碍物网格，其余的为自由网格。

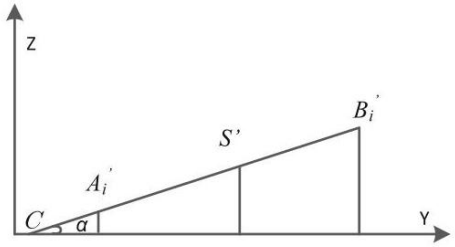

(a) Projection diagram in the case of a SID

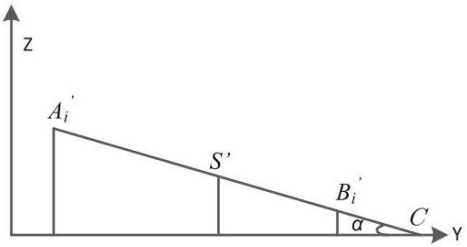

(b) Projection diagram in the case of a STAR

Fig. 3 Projection diagram of the S -plane on the YOZ -plane

图 3 S 平面在 YOZ 平面上的投影图

Step 4: Calculate the grid coordinates on the S -plane. First, make the following definition:

第四步: 计算 S 平面上的网格坐标。首先，做以下定义:

(1) The projection coordinate of the start point $A_i = \left({A_x}^i\ ,\ {A_y}^i, {A_z}^i\right)$ on the YOZ-plane is $A_i{}' = \left({A_y}^i, {A_z}^i\right)$;

(1) 起始点 $A_i = \left({A_x}^i\ ,\ {A_y}^i, {A_z}^i\right)$ 在 YOZ 平面的投影坐标是 $A_i{}' = \left({A_y}^i, {A_z}^i\right)$;

(2) The projection coordinate of the end point $B_i = \left({B_x}^i\ ,\ {B_y}^i, {B_z}^i\right)$ on the YOZ-plane is $B_i{}' = \left({B_y}^i, {B_z}^i\right)$;

(2) 终止点 $B_i = \left({B_x}^i\ ,\ {B_y}^i, {B_z}^i\right)$ 在 YOZ 平面的投影坐标是 $B_i{}' = \left({B_y}^i, {B_z}^i\right)$;

(3) The coordinate of the projection point of any point $S\ (S_x, S_y, S_z)$ on the YOZ-plane is $S'\ (S_y, S_z)$;

(3) YOZ 平面上任意点 $S\ (S_x, S_y, S_z)$ 的投影点的坐标是 $S'\ (S_y, S_z)$;

(4) The angle between the S -plane and the XOY -plane is α ;

(4) S 平面与 XOY 平面之间的角度是 α ;

(5) The extension line of the line A_i and B_i intersects the Y -axis at point C , where $C = (C_y, 0)$;

(5) 直线 A_i 和 B_i 的延长线在 Y 轴上的交点为 C ，其中 $C = (C_y, 0)$;

The start point and end point of the terminal routes contain two different heights, namely, the endpoint of a SID is higher than the start point, and the start point of a STAR is higher than the endpoint. In the case of a SID, the projection of start point, endpoint, S -plane, and any point on the S -plane on the YOZ-plane is shown in Fig. 3a. Similarly, in the case of a STAR, the projection diagram of the S -plane is shown in Fig. 3b.

起始点和终端路线的终点包含两个不同的高度，即 SID 的终点高于起点，STAR 的起点高于终点。在 SID 的情况下，起点的投影、终点的投影、S 平面以及该平面上任意点在 YOZ 平面上的投影如图 3a 所示。类似地，在 STAR 的情况下，S 平面的投影图如图 3b 所示。

As can be seen from Fig. 3, $\tan\alpha$ is the takeoff and descent gradient of the aircraft. In the case of the departure route:

从图 3 可以看出，$\tan\alpha$ 是飞机的起飞和降落梯度。在起飞路线的情况下:

$$\tan\alpha = \frac{B_z^i - A_z^i}{B_y^i - A_y^i} = \frac{B_z^i - S_z}{B_y^i - S_y} \tag{8}$$

Table 1 Obstacle coordinates and height

表 1 障碍物坐标及高度

Number	Longitude (°E)	Latitude (°N)	Height (m)	Number	Longitude (°E)	Latitude (°N)	Height (m)
1	103.97	30.67	572	21	103.96	30.54	539
2	103.97	30.62	548	22	103.97	30.51	553
3	103.96	30.60	542	23	103.95	30.53	545
4	104.06	30.66	642	24	103.94	30.52	528
5	103.98	30.60	553	25	103.94	30.50	569
6	103.96	30.59	551	26	103.94	30.46	579
7	104.06	30.61	595	27	103.94	30.45	565
8	104.08	30.58	589	28	103.94	30.51	544
9	103.95	30.58	560	29	103.93	30.50	539
10	104.06	30.56	617	30	103.93	30.51	540
11	104.07	30.55	628	31	103.92	30.48	580
12	103.96	30.57	549	32	103.93	30.47	541
13	104.06	30.50	576	33	103.92	30.50	541
14	103.98	30.54	578	34	103.93	30.52	535
15	103.98	30.52	573	35	103.92	30.51	541
16	103.98	30.53	559	36	103.93	30.53	551
17	103.98	30.52	555	37	103.91	30.50	562
18	103.95	30.57	580.4	38	103.91	30.51	556
19	103.96	30.51	539	39	103.90	30.49	568
20	103.96	30.54	554	40	103.90	30.48	586

编号	经度 (°E)	纬度 (°N)	高度 (m)	编号	经度 (°E)	纬度 (°N)	高度 (m)
1	103.97	30.67	572	21	103.96	30.54	539
2	103.97	30.62	548	22	103.97	30.51	553
3	103.96	30.60	542	23	103.95	30.53	545
4	104.06	30.66	642	24	103.94	30.52	528
5	103.98	30.60	553	25	103.94	30.50	569
6	103.96	30.59	551	26	103.94	30.46	579
7	104.06	30.61	595	27	103.94	30.45	565
8	104.08	30.58	589	28	103.94	30.51	544
9	103.95	30.58	560	29	103.93	30.50	539
10	104.06	30.56	617	30	103.93	30.51	540
11	104.07	30.55	628	31	103.92	30.48	580
12	103.96	30.57	549	32	103.93	30.47	541
13	104.06	30.50	576	33	103.92	30.50	541
14	103.98	30.54	578	34	103.93	30.52	535
15	103.98	30.52	573	35	103.92	30.51	541
16	103.98	30.53	559	36	103.93	30.53	551
17	103.98	30.52	555	37	103.91	30.50	562
18	103.95	30.57	580.4	38	103.91	30.51	556
19	103.96	30.51	539	39	103.90	30.49	568
20	103.96	30.54	554	40	103.90	30.48	586

Derive:
推导:

$$S_z = \tan\alpha \cdot \left(S_y - B_y^i\right) + B_z^i \tag{9}$$

In the case of the arrival route:
在到达路线的情况下:

$$\tan\alpha = \frac{A_z^i - B_z^i}{B_y^i - A_y^i} = \frac{S_z - B_z^i}{B_y^i - S_y} \tag{10}$$

Derive:
推导:

$$S_z = \tan\alpha \cdot \left(B_y^i - S_y\right) + B_z^i \tag{11}$$

After the S -plane is rasterized using Steps 3 and 4, the obstacles $\Omega_j = (x_j, y_j, z_j)$ in the 3D grid correspond to the coordinates $S(S_x, S_y, S_z)$ on the S -plane, and S_z can be obtained by formula (9) or formula (11). If S_z is greater than Z_j , the grid centered on $S(S_x, S_y, S_z)$ on the S -plane is a free grid, and vice versa is an obstacle grid. The size of the grid on the S -plane is $a \cdot (a/\cos\alpha)$.

在使用步骤 3 和 4 对 S -平面进行光栅化之后，3D 网格中的障碍物 $\Omega_j = (x_j, y_j, z_j)$ 对应于 S -平面上的坐标 $S(S_x, S_y, S_z)$ ，并且 S_z 可以通过公式 (9) 或公式 (11) 获得。如果 S_z 大于 Z_j ，则 S -平面上的以 $S(S_x, S_y, S_z)$ 为中心的网格是自由网格，反之则是障碍物网格。S -平面上的网格大小是 $a \cdot (a/\cos\alpha)$ 。

3.2 Solving STARs and SIDs planning model using A* algorithm

3.2 使用 A* 算法解决 STARs 和 SIDs 规划模型

There are several STARs and SIDs in TMA, and the planning order of the routes will have a direct impact on the economics of the routes. Our work adopts the planning principle based on flow descending: first plan the routes with large traffic, then plan the routes with small traffic, and the SID takes precedence over the STAR.

在 TMA 中有几个 STARs 和 SIDs，路由的规划顺序将直接影响路由的经济性。我们的工作采用了基于流量降序的规划原则: 首先规划流量大的路由，然后规划流量小的路由，并且 SID 优先于 STAR。

The essence of the A* algorithm [17, 18] is the combination of greedy algorithm and heuristic algorithm [19, 20], so the A* algorithm combines the advantages of these two algorithms and has high search efficiency in path planning problem. At the same time, the nature of the greedy algorithm that the A* algorithm has in the operation process can ensure that the optimal solution is found in the planning environment. If there is an optimal path from the start point to the end point in the planning environment, the reasonable heuristic function can be designed to find the optimal solution of the path in a short time. So the A* algorithm is selected to search for the optimal planning of STARs and SIDs on the above 2D grid S -plane. The unit grid on the 2D grid S -plane is used as the node searched by A* algorithm, and the implementation process of the A* algorithm is as follows:

A* 算法 [17, 18] 的本质是贪婪算法和启发式算法 [19, 20] 的结合，因此 A* 算法融合了这两种算法的优点，并在路径规划问题中具有高搜索效率。同时，A* 算法在操作过程中具有的贪婪算法特性可以确保在规划环境中找到最优解。如果在规划环境中存在从起点到终点的最优路径，可以设计合理的启发式函数，以快速找到路径的最优解。因此，选择 A* 算法来搜索上述二维网格 S 平面上的 STARs 和 SIDs 的最优规划。二维网格 S 平面上的单元网格被用作 A* 算法搜索的节点，A* 算法的实现过程如下:

Step 1: Design the A* algorithm cost function. The general expression of the A* algorithm cost function is:

第一步: 设计 A* 算法的成本函数。A* 算法成本函数的一般表达式为:

$$f(n) = g(n) + h(n) \tag{12}$$

In formula (12), $f(n)$ is the cost function of each node n , $g(n)$ is the cost from the start point to node n , and $h(n)$ is the cost of the node to the target node.

在公式 (12) 中，$f(n)$ 是每个节点 n 的成本函数，$g(n)$ 是从起点到节点 n 的成本，$h(n)$ 是节点到目标节点的成本。

On the 2D grid S -plane, the aircraft is located in any grid point and can move towards the current surrounding grids.

在二维网格 S 平面上，飞机位于任意网格点，并且可以朝向当前周围的网格移动。
Table 2 The coordinates of special use airspace areas
表 2 特殊使用空域区域的坐标

Name		Longitude (°E)	Latitude (°N)
ZPR407	1	103.17	31.43
	2	104.17	31.46
	3	104.17	30.71
	4	103.21	30.63
ZPR408	1	104.78	30.42
	2	105.30	30.43
	3	105.67	28.51
	4	105.50	28.53
ZPR420	1	103.21	30.63
	2	103.85	30.45
	3	104.09	29.92
	4	104.05	28.74
	5	103.50	28.50

名称		经度 (°E)	纬度 (°N)
ZPR407	1	103.17	31.43
	2	104.17	31.46
	3	104.17	30.71
	4	103.21	30.63
ZPR408	1	104.78	30.42
	2	105.30	30.43
	3	105.67	28.51
	4	105.50	28.53
ZPR420	1	103.21	30.63
	2	103.85	30.45
	3	104.09	29.92
	4	104.05	28.74
	5	103.50	28.50

Therefore, the distance between the grids is calculated by the Euclidean distance formula, that is:
因此，网格之间的距离是通过欧几里得距离公式计算的，即:

$$d = \sqrt{(x_1 - x_2)^2 + (y_1 - y_2)^2} \tag{13}$$

In formula (13), $(x_1, x_2), (y_1, y_2)$ are the coordinates of two points on the 2DS -plane, respectively, and d represents the distance between (x_1, x_2) and (y_1, y_2) .

在公式 (13) 中，$(x_1, x_2), (y_1, y_2)$ 分别是 2DS 平面上两点的坐标，d 表示 (x_1, x_2) 与 (y_1, y_2) 之间的距离。

Let the current node where the aircraft is located be p , the next node q of the node p has n candidates, $j = 1, 2, \ldots, n$. The spatial coordinates of the node q on the 2DS -plane are (q_x, q_y, q_z) , the start point coordinate of the route is $A_i = \left({A_x}^i, {A_y}^i, {A_z}^i\right)$, the end point coordinate of the route is $B_i = \left({B_x}^i, {B_y}^i, {B_z}^i\right)$. The cost function of the A* algorithm on the 2D S -plane is designed as Eq. (14)-(16):

设飞机当前位置的节点为 p ，节点 p 的下一个节点 q 有 n 个候选节点 $j = 1, 2, \ldots, n$ 。节点 q 在 2DS 平面上的空间坐标是 (q_x, q_y, q_z) ，航线的起点坐标是 $A_i = \left({A_x}^i, {A_y}^i, {A_z}^i\right)$ ，终点坐标是 $B_i = \left({B_x}^i, {B_y}^i, {B_z}^i\right)$ 。在二维 S 平面上，A* 算法的成本函数设计为公式 (14)-(16):

$$f(q) = g(q) + h(q) \tag{14}$$

$$g(q) = g(p) + \sqrt{(q_x - p_x)^2 + (q_y - p_y)^2 + (q_z - p_z)^2} \tag{15}$$

$$h(q) = \sqrt{(q_x - B_x^i)^2 + \left(q_x - B_y^i\right)^2 + (q_x - B_z^i)^2} \tag{16}$$

In the above formulas, $g(q)$ represents the cost of the route start point A_i to the node q, $g(p)$ represents the cost of the route start point A_i to the node p , and $h(q)$ represents the cost of the node q to the route end point B_i .

在上述公式中，$g(q)$ 表示航线起点 A_i 到节点 q, $g(p)$ 的成本，p 表示航线起点 A_i 到节点 $h(q)$ 的成本，q 表示节点 B_i 到航线终点的成本 [latex7] 。

Step 2: Start from the start point of the route, search for all nodes in the current neighborhood of the start point. Calculate $f(q)$ of all neighbor nodes to find the node with the smallest $f(q)$ value;

步骤 2: 从航线的起点开始，搜索起点当前邻域内的所有节点。计算所有邻节点的 $f(q)$ 值，以找到 $f(q)$ 值最小的节点；

Step 3: Take the node with the lowest value of $f(q)$ in Step 2 as the new start point of the route, continue to search the node with the lowest value of $f(q)$ in the neighborhood of the new start point until it reaches the terminal of the route.

translation: 步骤 3: 将步骤 2 中 $f(q)$ 值最小的节点作为航线的新起点，继续在新起点邻域内搜索 $f(q)$ 值最小的节点，直到达到航线的终点。

Step 4: Backtrack from the end point to the start point, connect all the nodes to form a route;

步骤 4: 从终点回溯到起点，连接所有节点形成航线；

Step 5: Plan routes one by one in order.

步骤 5: 按顺序逐一规划航线。

(1) First plan the departure route, then plan the arrival route. Since the fuel consumption of the aircraft is significantly greater at low altitude leveling and climbing than at high altitude, the aircraft needs to climb to cruise altitude as quickly as possible during the takeoff departure phase to avoid the increased fuel consumption at low altitude. While the approach aircraft descent generally uses engine idling, thrust is almost zero, and fuel consumption is minimal. When continuous descent techniques are used, the route length is no longer the limiting bottleneck for fuel reduction. Therefore, departure routes take precedence over arrival routes.

(1) 首先规划起飞离场航线，然后规划到达航线。由于飞机在低空平飞和爬升时的燃油消耗显著高于高空，飞机在起飞离场阶段需要尽快爬升到巡航高度，以避免在低空增加燃油消耗。而进近飞机下降通常使用发动机慢车，推力几乎为零，燃油消耗最小。当使用连续下降技术时，航线长度不再是燃油减少的限制瓶颈。因此，离场航线优先于到达航线。

(2) Based on satisfying the first principle, to minimize disruption to routes with high traffic volumes, the route with large traffic is prioritized.

(2) 在满足第一原则的基础上，为了最小化对高交通量航线的影响，优先考虑大流量航线。

(3) If the previously planned route passes the current 2D S -plane of the route to be planned, the grid through which

(3) 如果之前规划的航线穿过当前待规划航线的二维 S 平面，那么该航线穿过的格子

Table 3 The coordinates of start and end points of SIDs

表 3 SID 起点和终点的坐标

Runway number	SID	Start point		End point	
20L	γ_1	DER1	(103.95° E, 30.55° N)	ZYG	(104.68° E, 30.12° N)
20R	γ_2	DER2	(103.95° E, 30.60° N)	DOREX	(104.38° E, 31.25° N)
20L	γ_3	DER1	(103.95° E, 30.55° N)	LUGVO	(104.97° E, 30.91° N)
20R	γ_4	DER2	(103.95° E, 30.60° N)	CZH	(103.69° E, 30.65° N)

跑道编号	标准离场程序 (SID)	起点位置		终点位置	
20L	γ_1	DER1	(103.95° E, 30.55° N)	ZYG	(104.68° E, 30.12° N)
20R	γ_2	DER2	(103.95° E, 30.60° N)	DOREX	(104.38° E, 31.25° N)
20L	γ_3	DER1	(103.95° E, 30.55° N)	LUGVO	(104.97° E, 30.91° N)
20R	γ_4	DER2	(103.95° E, 30.60° N)	CZH	(103.69° E, 30.65° N)

Table 4 The coordinates of start and end points of STARs

表 4 STAR 起点和终点的坐标

Runway number	STAR	Start point		End point	
02L	$\gamma 5$	IAF1	(103.77° E, 30.04° N)	CZH	(103.69° E, 30.65° N)
02R	γ_6	IAF2	(103.95° E, 30.23° N)	FJC	(104.30° E, 29.93° N)
02R	11	IAF2	(103.95° E, 30.23° N)	TEB	(104.95° E, 30.67° N)

跑道编号	标准进近程序 (STAR)	起始点		终点	
02L	$\gamma 5$	初始进近定位点 1 (IAF1)	(103.77° 东经, 30.04° 北纬)	指定的五边形区域 (CZH)	(103.69° 东经, 30.65° 北纬)
02R	γ_6	初始进近定位点 2 (IAF2)	(103.95° 东经, 30.23° 北纬)	FJC	(104.30° E, 29.93° N)
02R	11	初始进近定位点 2 (IAF2)	(103.95° 东经, 30.23° 北纬)	TEB	(104.95° E, 30.67° N)

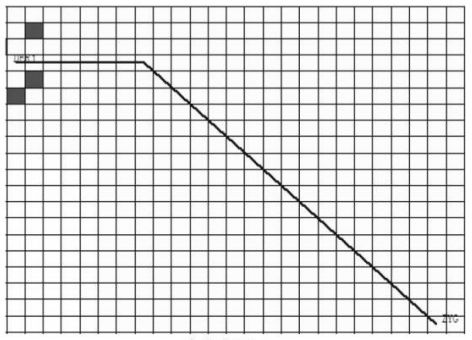

(a) SID γ_1

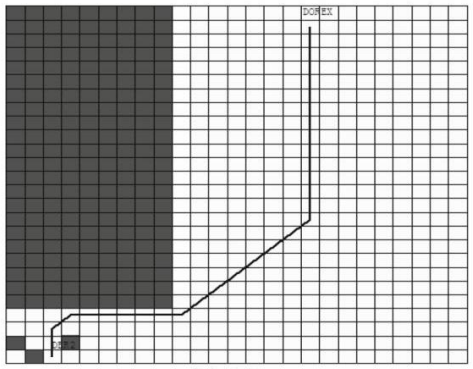

(b) SID γ_2

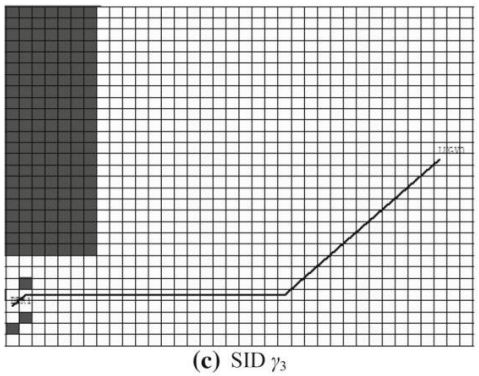

(c) SID γ_3

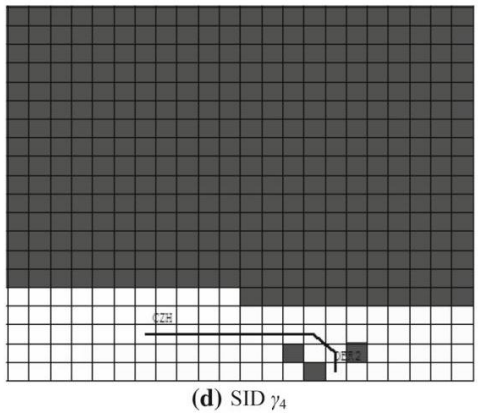

(d) SID γ_4

Fig. 4 SID planning results diagram (7% takeoff slope)
图 4 SID 规划结果图 (7% 起飞坡度)

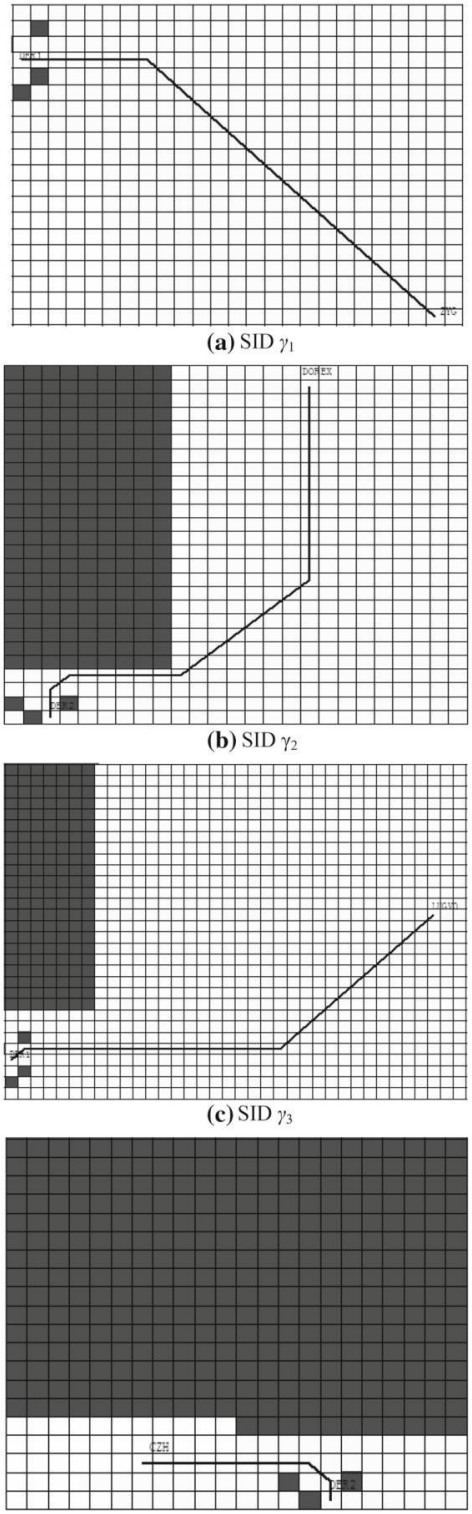

(a) SID γ_1

(b) SID γ_2

(c) SID γ_3

Fig. 5 SID planning results diagram (11% takeoff slope) the previously planned route passes is regarded as an obstacle grid to avoid the intersection between the routes.

图 5 SID 规划结果图 (11% 起飞坡度) 之前规划的航线穿过的格子被视为障碍格子，以避免航线之间的交叉。

Step 6: Complete the planning of all routes..

第 6 步: 完成所有航线的规划。

4 Simulation results

4 仿真结果

Take the runway of Chengdu Shuangliu Airport (ZUUU) as an example to carry out 3D planning of STARs and SIDs. The terrain in Chengdu TMA is complex, and there are many obstacles and special-use airspace areas. The airspace environment input data is as follows:

以成都双流机场 (ZUUU) 跑道为例进行 STARs 和 SIDs 的三维规划。成都管制区域 (TMA) 地形复杂，存在许多障碍物和特殊用途空域。空域环境输入数据如下:

(1) There are 103 obstacles in the Chengdu TMA, and only 40 obstacles affecting the flight procedure within the scope of departure and arrival points are considered. The obstacle coordinates and height are shown in Table 1.

(1) 成都 TMA 内有 103 个障碍物，仅考虑影响起飞和到达点范围内飞行程序的 40 个障碍物。障碍物坐标和高度如表 1 所示。

(2) Regarding the special use airspace areas in the Chengdu TMA, only three restricted areas that have an impact on the use of the runway are considered. They are ZPR407, ZPR408, and ZPR420 respectively, and all restricted areas are regarded as non-flying airspace. The coordinates of special use airspace areas are shown in Table 2.

(2) 关于成都终端区内的特殊使用空域，仅考虑了三个对跑道使用有影响的限制区域，分别是 ZPR407、ZPR408 和 ZPR420，所有这些限制区域都被视为禁飞空域。特殊使用空域的坐标如表 2 所示。

(3) The runway numbers are 02 L, 20R, 20 L , and 02R , respectively, and the length of both runways is 3600 m .

(3) 跑道的编号分别为 02 L, 20R, 20 L 和 02R ，两条跑道的长度均为 3600 m 。

(4) The SIDs to be planned are, respectively, $\gamma_1, \gamma_2, \gamma_3$, and γ_4 , and the coordinates of start and end points are shown in Table 3.

(4) 计划中的起飞爬升航迹分别为 $\gamma_1, \gamma_2, \gamma_3$ 和 γ_4 ，起点和终点的坐标如表 3 所示。

(5) The STARs to be planned are, respectively, γ_5, γ_6 , and γ_7 , and the coordinates of start and end points are shown in Table 4.

(5) 计划中的标准到达航迹分别为 γ_5, γ_6 和 γ_7 ，起点和终点的坐标如表 4 所示。

(6) Takeoff slopes $\alpha_{\min,\mathrm{TO}} = 7\% (\sim 4\mathrm{deg})$, $\alpha_{\max,\mathrm{TO}} = 11\% (\sim 6.3\mathrm{deg})$; Descent slopes $\alpha_{\min,\mathrm{LD}} = 1.6\% (\sim 0.92\mathrm{deg})$, $\alpha_{\max,\mathrm{LD}} = 4.2\% (\sim 2.4\mathrm{deg})$.

(6) 起飞坡度 $\alpha_{\min,\mathrm{TO}} = 7\% (\sim 4\mathrm{deg})$, $\alpha_{\max,\mathrm{TO}} = 11\% (\sim 6.3\mathrm{deg})$;下降坡度 $\alpha_{\min,\mathrm{LD}} = 1.6\% (\sim 0.92\mathrm{deg})$, $\alpha_{\max,\mathrm{LD}} = 4.2\% (\sim 2.4\mathrm{deg})$ 。

Using the method described in Sect. 3.1, the airspace environment of ZUUU is rasterized. Considering the horizontal interval between aircraft, it is divided into $60 * 60 * 60$ grids, each grid size is 3 km . Due to the different takeoff/descent slopes of the departure route and the arrival route, two schemes are planned for each route according to the maximum and minimum takeoff/descent slopes. The aircraft can use any route between the height ranges of the two schemes. According to the route planning priority principle (the SID takes precedence over the STAR, the route with large traffic takes precedence over the route with small traffic), the route planning sequence is $\gamma_1 > \gamma_2 > \gamma_3 > \gamma_4 > \gamma_5 > \gamma_6 > \gamma_7$, and the routes are planned separately in different 2D grid S -plane generated after dimensionality reduction. The simulation results are as follows:

使用第 3.1 节中描述的方法，将 ZUUU 的空域环境栅格化。考虑到飞机之间的水平间隔，将其划分为 $60 * 60 * 60$ 个格子，每个格子的大小为 3 km 。由于出发航路和到达航路的起飞/下降坡度不同，根据最大和最小起飞/下降坡度，为每条航路规划了两个方案。飞机可以在两个方案的高度范围内使用任意航路。根据航路规划优先原则 (SID 优先于 STAR，流量大的航路优先于流量小的航路)，航路规划顺序为 $\gamma_1 > \gamma_2 > \gamma_3 > \gamma_4 > \gamma_5 > \gamma_6 > \gamma_7$ ，并在降维后生成的不同 2D 格子 S 平面上分别规划航路。模拟结果如下:

A. If according to the 7% takeoff slope, the planning result of the SID $\gamma_1, \gamma_2, \gamma_3, \gamma_4$ is shown in Fig. 4; If according to the 11% takeoff slope, the planning results of the SID $\gamma_1, \gamma_2, \gamma_3, \gamma_4$ are shown in Fig. 5 shows.

A. 如果根据 7% 起飞斜率，SID $\gamma_1, \gamma_2, \gamma_3, \gamma_4$ 的规划结果如图 4 所示；如果根据 11% 起飞斜率，SID $\gamma_1, \gamma_2, \gamma_3, \gamma_4$ 的规划结果如图 5 所示。

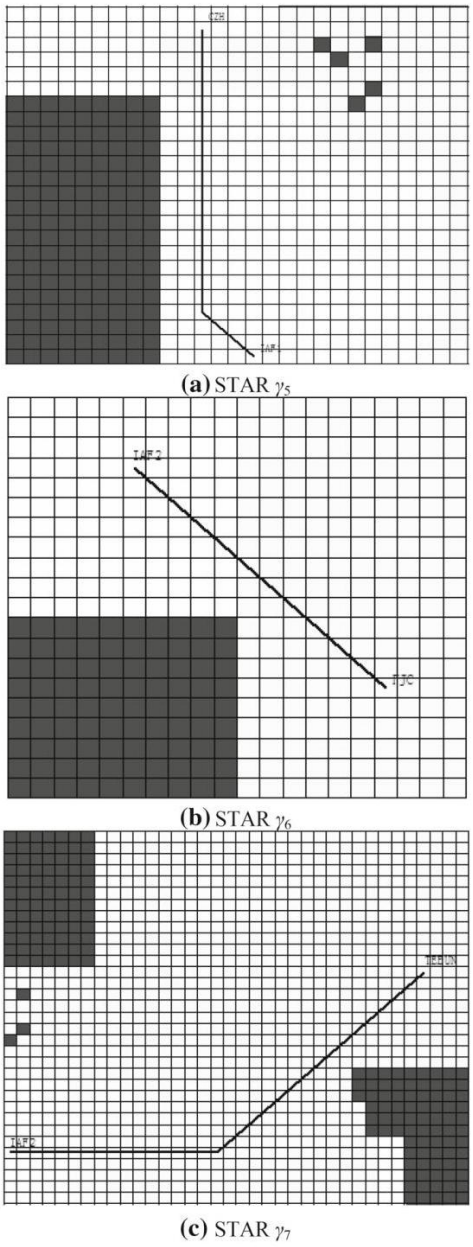

(a) STAR γ_5

(b) STAR γ_6

(c) STAR γ_7

Fig. 6 STAR planning results diagram (1.6% descent slope)

图 6 STAR 规划结果图 (1.6% 下降斜率)

B. If according to the 1.6% descent slope, the planning results of the STAR $\gamma_5, \gamma_6, \gamma_7$ are shown in Fig. 6; If according to the 4.2% descent slope, the planning results of the STAR $\gamma_5, \gamma_6, \gamma_7$ are shown in Fig. 7.

B. 如果根据 1.6% 下降斜率，STAR $\gamma_5, \gamma_6, \gamma_7$ 的规划结果如图 6 所示；如果根据 4.2% 下降斜率，STAR $\gamma_5, \gamma_6, \gamma_7$ 的规划结果如图 7 所示。

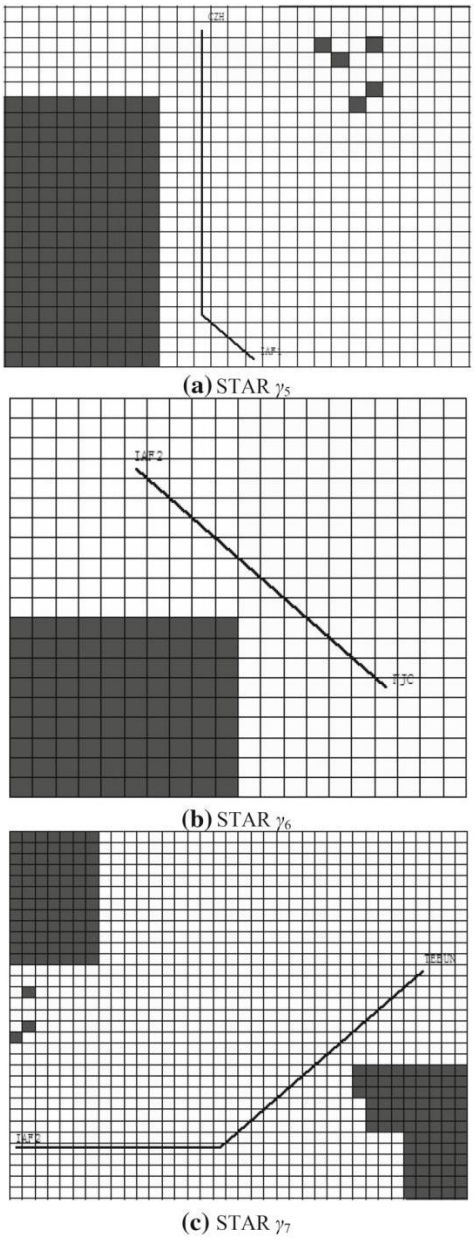

(a) STAR γ_5

(b) STAR γ_6

(c) STAR γ_7

Fig. 7 STAR planning results diagram (4.2% descent slope)

图 7 STAR 规划结果图 (4.2% 下降斜率)

In Figs. 4, 5, 6, 7, Figs. 4 and 5 have the same obstacle grids, and Figs. 6 and 7 have the same obstacle grids, so 7% take-off slope and 11% take-off slope have the same floor plans, and 1.6% descent slope and 4.2% descent slope have the same plan, but the length and height of each route are different. In addition, the grid sizes in Figs. 4, 5, 6, 7 are different, respectively, $3\text{ km} * (3/\cos 4^\circ)\text{ km}, 3\text{ km} * (3/\cos 6.3^\circ)$ $\text{km}, 3\text{ km} * (3/\cos 0.92^\circ)\text{ km}, 3\text{ km} * (3/\cos 2.4^\circ)\text{ km}$.

在图 4、5、6、7 中，图 4 和 5 具有相同的障碍物网格，图 6 和 7 具有相同的障碍物网格，因此 7% 起飞斜率和 11% 起飞斜率具有相同的平面图，1.6% 下降斜率和 4.2% 下降斜率具有相同的规划，但每条路线的长度和高度各不相同。此外，图 4、5、6、7 中的网格大小分别不同，分别为 $3\text{ km} * (3/\cos 4^\circ)\text{ km}, 3\text{ km} * (3/\cos 6.3^\circ)$ $\text{km}, 3\text{ km} * (3/\cos 0.92^\circ)\text{ km}, 3\text{ km} * (3/\cos 2.4^\circ)\text{ km}$ 。

The planning effect of the traditional grid method is compared with the planning effect of using the high dimensionality reduction environment modeling method. The route planning results of the two methods are shown in Table 5.

将传统网格方法的规划效果与使用高维度降低环境建模方法的规划效果进行比较。两种方法的路线规划结果如表 5 所示。

Table 5 shows the data for each route, including the takeoff/descent slope for each route, the height of

the start and end points, and the length of the route. Under different takeoff and descent slopes, the 3D path planning length of each route is longer than the path planning length in the 2D plane environment with high dimensionality reduction, and the route planning time in the 2D environment is less than that in the 3D environment. It can be seen that for the planning algorithm, the modeling environment processed by the high dimensionality reduction method has higher processing efficiency and better route planning results than the traditional grid method.

表 5 显示了每条路线的数据，包括每条路线的起飞/降落坡度、起点和终点的海拔高度以及路线的长度。在不同的起飞和降落坡度下，每条路线的三维路径规划长度均大于在二维平面环境中进行路径规划时的长度，且在 2D 环境中的路线规划时间小于在三维环境中的规划时间。可以看出，对于规划算法来说，使用高维度降低方法处理的建模环境比传统网格方法具有更高的处理效率和更好的路线规划结果。

C. Draw 3d planning results of all routes, as shown in Fig. 8.

C. 绘制所有路线的三维规划结果，如图 8 所示。

In Fig. 8, the departure route $\gamma_1, \gamma_2, \gamma_3, \gamma_4$ is represented by a blue line, the arrival route $\gamma_5, \gamma_6, \gamma_7$ is represented by a red line, the obstacle is represented by a small black solid cube, and the special use airspace area is represented by a yellow transparent cube. Each SID/STAR has a route under the maximum and minimum takeoff/descent profiles, and the two routes are connected by black dashed lines to form a cone that contains all ascent (or descent) profiles of the aircraft. The departure route/arrival route has no contact with obstacles and special-use airspace areas in the TMA, and there is no route cross between the departure route and the arrival route. The arrival route γ_7 and the departure route γ_2, γ_3 seem to have intersections in Fig. 8, but in fact, they are staggered in height.

在图 8 中，出发路线 $\gamma_1, \gamma_2, \gamma_3, \gamma_4$ 用蓝色线表示，到达路线 $\gamma_5, \gamma_6, \gamma_7$ 用红色线表示，障碍物用小黑色实心立方体表示，特殊用途空域区域用黄色透明立方体表示。每个 SID/STAR 在最大和最小起飞/降落剖面下都有一个对应的路线，这两条路线通过黑色虚线连接，形成一个包含飞机所有上升 (或下降) 剖面的圆锥。出发路线/到达路线在 TMA 内不与障碍物和特殊用途空域区域接触，且出发路线与到达路线之间不存在路线交叉。虽然在图 8 中到达路线 γ_7 和出发路线 γ_2, γ_3 看起来有交点，但实际上它们在高度上是错开的。

5 Conclusion

5 结论

The STARs and SIDs of the TMA serve as an important route to guide the takeoff and landing of aircraft, = and are an important foundation to guarantee the safety and operational efficiency of air traffic operations. In this paper, we aim to solve the 3D planning problem of the STARs and SIDs, and establish the STARs and SIDs planning model with the minimum route length as the objective while taking into account operational and environmental constraints: in particular, aircraft's turning angle, aircraft's takeoff and descent slope, obstacle and special-use airspace area avoidance. To reduce the complexity of the model and improve the efficiency of the algorithm, we use a rasterized 3D environment modeling method based on high dimensionality reduction to process the airspace environment in TMA, and then use the A* algorithm to generate the terminal routes sequentially in the airspace environment after dimensionality reduction according to the principle of route planning. The proposed methodology is applied to design terminal routes in TMA of ZUUU in China. A total of 7 routes are designed, including 4 SIDs and 3 STARs. A planning scheme is given for each route under the maximum and minimum takeoff/descent slope, and the aircraft could fly on any route between the two planning schemes. The planned routes are continuous and approximately smooth, there is no intersection between the routes, and the angle at any turning point meets the aircraft turning constraint. Compared with the traditional raster method, the route planning in the dimensionality reduction environment has higher planning efficiency and shorter route length. The experimental results show that the proposed method is effective and can be regarded as a decision support tool for the design of STARs and SIDs.

TMA 的 STARs 和 SIDs 作为指导飞机起飞和降落的重要航线 = ，并且是确保空中交通运行安全和运营效率的重要基础。在本文中，我们旨在解决 STARs 和 SIDs 的 3D 规划问题，并建立以最小航线长度为目标，同时考虑运行和环境约束的 STARs 和 SIDs 规划模型: 特别是飞机的转弯角度、飞机的起飞和下降坡度、障碍物和特殊用途空域的规避。为了降低模型复杂性和提高算法效率，我们使用基于高维

度降低的栅格化 3D 环境建模方法来处理 TMA 的空域环境，然后根据航线规划的原则，在降维后的空域环境中使用 A* 算法依次生成终端航线。提出的方法应用于中国 ZUUU 机场 TMA 的终端航线设计。共设计了 7 条航线，包括 4 条 SIDs 和 3 条 STARs。在每个航线的最大和最小起飞/下降坡度下，都给出了规划方案，飞机可以在两个规划方案之间的任何航线上飞行。规划的航线连续且近似平滑，航线之间没有交叉，且任何转弯点的角度都满足飞机的转弯约束。与传统栅格方法相比，降维环境中的航线规划具有更高的规划效率和更短的航线长度。实验结果表明，提出的方法是有效的，可以作为设计 STARs 和 SIDs 的决策支持工具。

Table 5 Comparison of route planning results of the two methods

表 5 两种方法航线规划结果的比较

Route	Takeoff/descent slope (%)	Start point	Start point height (km)	End point	End point heigh (km)	(High dimensionality reduction method) Route length (km)	(Traditional grid method) Route length (km)
γ_1	7	DER1	0	ZYG	5.86	83.91	98.85
	11	DER1	0	ZYG	9.2	84.76	100.23
γ_2	7	DER2	0	DOREX	5.75	83.31	103.65
	11	DER2	0	DOREX	9	83.60	105.45
γ_3	7	DER1	0	LUGVO	7.38	105.74	118.24
	11	DER1	0	LUGVO	11.6	106.11	120.15
γ_4	7	DER2	0	CZH	2	27.48	35.89
	11	DER2	0	CZH	3	27.58	37.64
Y5	1.6	CZH	3.5	IAF1	2.4	66.60	77.22
	4.2	CZH	5.2	IAF1	2.4	66.66	78.12
γ_6	1.6	FJC	2.24	IAF2	1.5	46.61	59.16
	4.2	FJC	3.5	IAF2	1.5	46.64	60.36
$\gamma 7$	1.6	TEB	3.2	IAF2	1.5	107.02	135.36
	4.2	TEB	6	IAF2	1.5	107.11	137.58

路线	起降坡度 (%)	起始点	起始点高度 (公里)	终点	终点高度 (公里)	(高维降维方法) 路线长度 (公里)	(传统网格方法) 路线长度 (公里)
γ_1	7	DER1	0	ZYG	5.86	83.91	98.85
	11	DER1	0	ZYG	9.2	84.76	100.23
γ_2	7	DER2	0	DOREX	5.75	83.31	103.65
	11	DER2	0	DOREX	9	83.60	105.45
γ_3	7	DER1	0	LUGVO	7.38	105.74	118.24
	11	DER1	0	LUGVO	11.6	106.11	120.15
γ_4	7	DER2	0	CZH	2	27.48	35.89
	11	DER2	0	CZH	3	27.58	37.64
Y5	1.6	CZH	3.5	IAF1	2.4	66.60	77.22
	4.2	CZH	5.2	IAF1	2.4	66.66	78.12
γ_6	1.6	FJC	2.24	IAF2	1.5	46.61	59.16
	4.2	FJC	3.5	IAF2	1.5	46.64	60.36
$\gamma 7$	1.6	TEB	3.2	IAF2	1.5	107.02	135.36
	4.2	TEB	6	IAF2	1.5	107.11	137.58

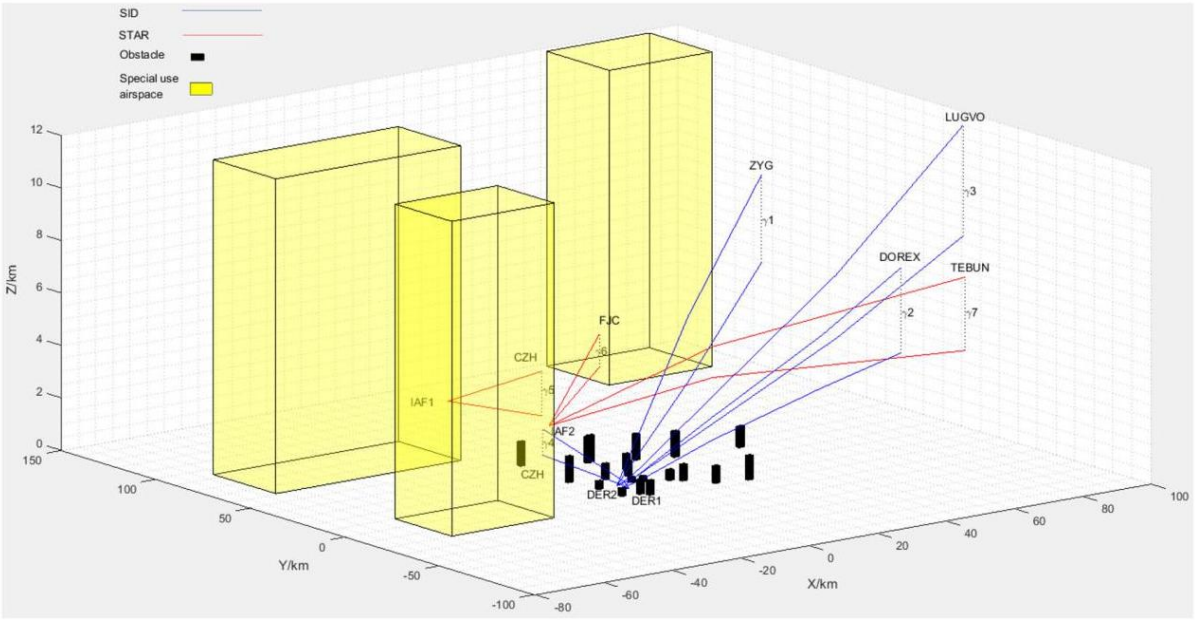

Fig. 8 3D diagram of route planning

图 8 航线规划的 3D 示意图

The next research work will optimize the location of the arrival and departure points based on the traffic flow allocation, and more rationally allocate the arrival point of the STAR and the departure point of the SID. Besides, the problem of avoiding dynamic obstacles in the airspace environment is also the focus of research in the next phase, making the planning of STARs and SIDs closer to the actual operating environment. Science and Technology Major Project (2017-VIII-0003-0114, 2017- VIII-0002), and Fundamental Research Funds for the Central Universities (56XBA18201, XBC20018, 56XBC18206).

下一项研究工作将基于交通流量分配优化起飞和降落点的位置，并更加合理地分配 STAR 的到达点和 SID 的起飞点。此外，下一阶段研究的重点还包括在空域环境中避开动态障碍物的问题，使得 STAR 和 SID 的规划更接近实际运行环境。科学技术重大专项 (2017-VIII-0003-0114，2017-VIII-0002) 以及中央高校基本科研业务费 (56XBA18201，XBC20018，56XBC18206)。

Data availability The data used to support the findings of this study are included in the article.

数据可用性支持本研究发现的原始数据包含在本文中。

Compliance with ethical standards

遵守道德标准

Conflict of interest We declare that we have no financial and personal relationships with other people or organizations that can inappropriately influence our work, there is no professional or other personal interest of any nature or kind in any product, service and/or company that could be construed as influencing the position presented in, or the review of, the manuscript entitled.

利益冲突我们声明，我们与其他个人或组织没有经济上或个人上的关系，这些关系可能会不适当地影响我们的工作。对于任何产品、服务和/或公司，我们没有任何专业或其他个人利益，这些利益可能会被认为影响到了本文的立场或审查。

References

参考文献

1. Eele A, Richards A (2009) Path planning with avoidance using nonlinear branch and bound optimization. J Guid Control Dyn 32(2):384-394. https://doi.org/10.2514/1.40034

2. Munoz P, Barrero DF, R-Moreno MD (2015) A statistically rigorous analysis of 2D path-planning algorithms. Comput J 58(11):2876-2891. https://doi.org/10.1093/comjnl/bxu137

3. Han J (2015) An efficient approach to 3D path planning. Inf Sci 478:318-330. https://doi.org/10.1016/j.ins.2018.11.0

4. Wang XY, Zhang GX, Zhao JB et al (2015) A Modified membrane-inspired algorithm based on particle swarm optimization for mobile robot path planning. Int J Comput Commun Control 10(5):732–745. https://doi.org/10.15837/ijccc.2015.5.2030

5. Kim DS, Yu K, Cho Y, Kim D et al (2004) Shortest Paths for disc obstacles. Comput Sci Appl. https://doi.org/10.1007/978-3-540-2 4767-8_7

6. GianazzaD, DurandN (2004) Separating air traffic flows by allocating 3-D-Trajectories. In: Digital Avionics Systems Conference.IEEE. doi: https://doi.org/10.1109/DASC.2004.1391275

7. Gallina P, Gasparetto A (2000) A technique to analytically formulate and to solve the 2-dimensional constrained trajectory planning problem for a mobile robot. J Intell Rob Syst 27(3):237-262. https://doi.org/10.1016/0149-1970(95)00097-6

8. SouissiO, BenatitallahR, DuvivierD, etal (2013). Path planning: a 2013 survey. In: International Conference on Industrial Engineering and Systems Management. IEEE.

9. Delahaye D, Puechmorel S, Tsiotras P et al (2014) Mathematical models for aircraft trajectory design: a survey. Lect Notes Elect Eng. https://doi.org/10.1007/978-4-431-54475-3_12

10. Pfeil DM (2011) Optimization of airport terminal-area air traffic operations under uncertain weather conditions. Massachusetts Institute of Technology, Cambridge

11. ZhouJ, CafieriS, DelahayeD, et al(2014) Optimization of arrival and departure routes in terminal maneuvering area.Int Conf Res Air Transp

12. Wang C, He CN, Liu HZ (2014) 3D Optimization method for terminal arrival and departure route network. Sci Technol Eng 14(11):81-85 (in Chinese)

13. He CN, Wang C, Jiang YQ (2014) 3D optimization for arrival and departure route network based on improved A* algorithm. Aeron Comput Tech 44(01):45-47+51 (in Chinese)

14. ZhouJ, CafieriS, DelahayeD, et al (2015). Optimizing the design of a route in terminal maneuvering area using branch and bound. In: ENRI International Workshop on ATM/CNS(EIWAC2015),

Acknowledgments This work was financially supported in part by the National Natural Science Foundation of China (U1333119), National

致谢本研究的部分经费得到了中国国家自然科学基金 (U1333119) 的支持，国家

Electronic Navigation Research Institute (ENRI) PaperEN-A-012. doi: https://doi.org/10.1007/978-4-431-56423-2_9

15. ZhouJ, CafieriS, DelahayeD, et al(2016)Optimal design of SIDs/STARs in TMA using simulated annealing. In: Digital Avionics Systems Conference. IEEE. doi: https://doi.org/10.1109/DASC.2016.7778099

16. Wang SJ, Cao X, Li HY et al (2017) Air route network optimization in fragmented airspace based on cellular automata. Chin J Aeronaut 30(3):1184-1195. https://doi.org/10.1016/j.cja.2017.04.002

17. Kala R, Shukla A, Tiwari R (2010) Fusion of probabilistic A*algorithm and fuzzy inference system for robotic path planning. Artif Intell Rev 33(4):307-327. https://doi.org/10.1007/s10462-01 0-9157-y

18. Ye X, Han SP, Lin A (2017) A note on the connection between the primal-dual and the A* algorithm. Int J Oper Res Inform Syst 1(1):73-85. https://doi.org/10.4018/joris.2010101305

19. Carmine C, Raffaele C, Bruce G (2017) Carousel greedy: a generalized greedy algorithm with applications in optimization. Comput Oper Res 85:97-112. https://doi.org/10.1016/j.cor.2017.03.016

20. Takafumi M (2018) A heuristic search algorithm based on subspaces for PageRank computation. J Supercomput 74(4):3278-3294. https://doi.org/10.1007/s11227-018-2383-9